MODELING OF THE SAWTOOTH INSTABILITY IN TOKAMAKS USING A CURRENT VISCOSITY TERM

D.J. Ward and S.C. Jardin

Plasma Physics Laboratory, Princeton University
Princeton, New Jersey 08543

ABSTRACT

We propose a new method for modeling the sawtooth instability and other MHD activity in axisymmetric tokamak transport simulations. A hyper-resistivity (or current viscosity) term is included in the mean field Ohm's law to describe the effects of the three-dimensional fluctuating fields on the evolution of the inverse transform, q, characterizing the mean fields. This term has the effect of flattening the current profile, while dissipating energy and conserving helicity. A fully implicit MHD transport and 2-D toroidal equilibrium code has been developed to calculate the evolution in time of the q-profile and the current profile using this new term. The results of this code are compared to the Kadomtsev reconnection model in the circular cylindrical limit.

1

MASTER

I. INTRODUCTION

   Tokamak transport simulation codes presently play an active and important role in magnetic fusion research. These codes have proved useful not as methods for predicting plasma behavior from first principles, but rather as lower dimensional reduced descriptions which enforce the appropriate conservation equations. They also account for fine scale or fluctuating three-dimensional phenomena by means of 'anomalous' coefficients or heuristically motivated prescriptions.

   One such class of phenomena which is essential to model at some level is the sawtooth instability [1]. There are presently several approaches used in doing this. One approach [2] is to incorporate the Kadomtsev complete reconnection model [3] at time intervals which are either predetermined or are linked in some way to the plasma evolution. Another method [4,5] used is to flatten the resistivity profile in the interior of the magnetic surface which has $q = 1$.

   Each of these prescriptions has some merit, but each also has some inconsistencies. The Kadomtsev model is only strictly applicable to a cylindrical plasma of circular cross section where a pure helical mode can exist. Even then, there is no guarantee that the helical structure would fully reconnect as assumed by this model. The resistivity flattening model does not explicitly conserve magnetic helicity as would be done by the underlying MHD instability.

   This paper deals with a new method for modeling the sawtooth instability in a tokamak transport code, based on introducing a hyper-resistivity or current viscosity term in the transport equations. It has been shown by several authors [6–9] that the effects of three-dimensional MHD fluctuations on the force-free mean field of a plasma can be represented by the introduction of a new term with one free parameter into Ohm's law such that

$$\vec{E} + \vec{v} \times \vec{B} = \eta_\parallel \vec{J}_\parallel + \eta_\perp \vec{J}_\perp - \frac{\vec{B}}{B^2}\vec{\nabla} \cdot \{[\lambda\vec{\nabla}(\frac{\vec{J}\cdot\vec{B}}{B^2})] - [\vec{u} \times \vec{\nabla}(\frac{\vec{J}\cdot\vec{B}}{B^2})]\}, \quad (1)$$

where λ is an arbitrary, positive function of position, and where $\vec{u}$ is an arbitrary vector function of position that may be chosen according to mathematical convenience. The form of the function λ has been calculated explicitly for tearing modes in the reversed-field pinch (RFP) [10,11] where hyper-resistivity is shown to sustain the magnetic field reversal and to produce plasmas near the force-free Taylor state [10,12]. Here, however, we make use only of the fact that an arbitrary, positive λ follows from the derivation in Ref. [9].

   The new term conserves magnetic helicity. Equation (1) is, in fact, the unique form of a force-free mean field Ohm's law under the assumptions [9]: (1) the exact magnetic field energy and helicity are closely approximated by the energy and helicity of the mean field, (2) the fluctuating field can cause differential transport of both the field energy and helicity, and (3) the fluctuating field can lead to enhanced dissipation of field energy but

2

not of field helicity. The underlying physical instabilities leading to sawtooth oscillations should satisfy these assumptions; therefore we propose to model sawteeth and other 3-D MHD phenomena using this equation in such an MHD transport model.

II. THEORY

It can be shown [13] that in a toroidal system with nested magnetic surfaces, the q-profile (safety factor profile) develops in time according to

$$\frac{\partial}{\partial t} q^{-1} = \frac{d}{d\Phi} V_L, \tag{2}$$

where Φ is the toroidal flux contained inside the $\Phi = constant$ surface, and $V_L(\Phi)$ is the loop voltage, defined by

$$V_L = \frac{2\pi <\mathcal{J}\vec{B}\cdot\vec{R}>}{<\mathcal{J}\vec{B}\cdot\vec{\nabla}\phi>}.$$

Angle brackets denote the flux surface average, defined by

$$<a> = \frac{1}{2\pi} \int_0^{2\pi} a \, d\theta.$$

Here $\vec{R}$ represents the right-hand side of Eq. (1), which can be written

$$\vec{E} + \vec{v} \times \vec{B} = \vec{R} = \vec{R}_C + \vec{R}_H,$$

and the Jacobian, $\mathcal{J}$, of the (Φ, θ, ϕ) magnetic flux coordinate system is defined by

$$\mathcal{J} = [\vec{\nabla}\Phi \times \vec{\nabla}\theta \cdot \vec{\nabla}\phi]^{-1}. \tag{3}$$

Here ϕ represents the axisymmetric toroidal angle with $|\nabla\phi|^2 = R^{-2}$, θ is the poloidal angle, and (R,ϕ,Z) are conventional cylindrical coordinates.

If we first consider only the classical term, $\vec{R}_C = \eta_\parallel \vec{J}_\parallel + \eta_\perp \vec{J}_\perp$, the loop voltage appearing in Eq. (2) is

$$V_L^{class} = 2\pi \, \eta_\parallel \, \frac{<\mathcal{J}\vec{J}\cdot\vec{B}>}{<\mathcal{J}\vec{B}\cdot\vec{\nabla}\phi>} = \frac{2\pi\eta_\parallel(g(\Phi))^2}{\mu_0} \, \frac{d}{d\Phi}\left(\frac{<|\nabla\Phi|^2 \frac{\mathcal{J}}{R^2}>}{g(\Phi)} \, q^{-1}\right). \tag{4}$$

We have taken the axisymmetric (or mean) magnetic field to be represented in the usual way,

3

$$\vec{B} = \vec{\nabla}\phi \times \vec{\nabla}\Psi + g(\Phi)\vec{\nabla}\phi, \tag{5}$$

with Ψ being the poloidal magnetic flux per radian, $\vec{\nabla}\Psi = (2\pi q)^{-1}\vec{\nabla}\Phi$, and g the toroidal field function, $g(\Phi) = [2\pi <\frac{\mathcal{J}}{R^2}>]^{-1}$.

Next consider the new term in the mean field Ohm's law that describes the effects of the 3-D turbulent field. The hyper-resistivity term is

$$\vec{R}_H = -\frac{\vec{B}}{B^2}\vec{\nabla}\cdot[(\lambda\vec{\nabla}\sigma) - (\vec{u}\times\vec{\nabla}\sigma)], \tag{6}$$

where,

$$\sigma = \frac{\vec{J}\cdot\vec{B}}{B^2} = \frac{g^2(\Phi)}{\mu_0 B^2 \mathcal{J}}\{\frac{\partial}{\partial\Phi}[\frac{\mathcal{J}|\nabla\Phi|^2}{R^2}\frac{1}{g(\Phi)}\Psi'] + \frac{\partial}{\partial\theta}[\frac{\mathcal{J}(\vec{\nabla}\theta\cdot\vec{\nabla}\Phi)}{R^2}\frac{1}{g(\Phi)}\Psi']\}, \tag{7}$$

the prime denoting differentiation with respect to Φ.

We take advantage of the fact that $\vec{u}$ can be any arbitrary function of position, and specify the form for $\vec{u}$ such that the terms with theta derivatives of σ cancel, thus

$$\vec{u} = -\lambda\mathcal{J}(\vec{\nabla}\Phi\cdot\vec{\nabla}\theta)\vec{\nabla}\phi. \tag{8}$$

The loop voltage corresponding to the hyper-resistivity term, Eq. (6), then becomes

$$V_L^H = 2\pi\frac{<\mathcal{J}\vec{B}\cdot\vec{R}_H>}{<\mathcal{J}\vec{B}\cdot\vec{\nabla}\phi>} = -(2\pi)^2\frac{\partial}{\partial\Phi}<\lambda\mathcal{J}|\nabla\Phi|^2\frac{\partial\sigma}{\partial\Phi}>. \tag{9}$$

Considerable simplification can be obtained by restricting the form of λ, the arbitrary function of position appearing in Eq. (1), to be of the form

$$\lambda = \frac{\Lambda(\Phi)}{(2\pi)^2\mathcal{J}|\nabla\Phi|^2}, \tag{10}$$

where $\Lambda(\Phi)$ is an arbitrary function of toroidal flux. In addition, we choose the angle θ in the (Φ, θ, ϕ) flux coordinate system so that the Jacobian, $\mathcal{J}$, is given by the Boozer form [14]

$$\mathcal{J} = \frac{f(\Phi)}{\mu_0 B^2},$$

where

$$f(\Phi) \equiv \frac{\mu_0}{(2\pi)^2<B^{-2}>}\frac{dV}{d\Phi},$$

4

$V(\Phi)$ being the volume enclosed by the flux surface with label Φ.

Including the loop voltage due to the classical term, Eq. (4), and that due to the hyper-resistivity term, Eq. (9), in the time evolution equation for q, Eq. (2), gives the final form for the complete equation to advance q in time relative to surfaces of constant toroidal flux

$$\frac{\partial}{\partial t}q^{-1} = \frac{d}{d\Phi}\left[\frac{2\pi\eta_{\parallel}(\Phi)}{\mu_0}(g(\Phi))^2\frac{d}{d\Phi}\left(\frac{<|\nabla\Phi|^2\frac{\mathcal{J}}{R^2}>}{g(\Phi)}q^{-1}\right)\right] \tag{11}$$

$$- \frac{d^2}{d\Phi^2}\left\{\left(\Lambda(\Phi)\frac{d}{d\Phi}\left(\frac{g^2(\Phi)}{f(\Phi)}\frac{d}{d\Phi}\left[\frac{<|\nabla\Phi|^2\frac{\mathcal{J}}{R^2}>}{g(\Phi)}q^{-1}\right]\right)\right)\right\}.$$

Equation (11) includes classical resistive field diffusion, as well as the new term representing the effect of the 3-D turbulent fields. We model sawteeth with this equation by evolving the q-profile in time with the resistive term only. When some threshold is reached (e.g., q_0 reaches some minimum value), we 'trigger' the sawtooth by turning on the hyper-resistivity term within some inner radius of the cross section.

As a first test of this model we consider the large aspect ratio cylindrical tokamak limit. The evolution equation, Eq. (11), becomes the simpler 1-D equation:

$$\frac{\partial\Psi}{\partial t} = \frac{\eta(r)}{\mu_0}\frac{1}{r}\frac{\partial}{\partial r}\left(r\frac{\partial\Psi}{\partial r}\right) - \frac{1}{r}\frac{\partial}{\partial r}(\bar{\lambda}r)\frac{\partial}{\partial r}\left[\frac{1}{r}\frac{\partial}{\partial r}r\frac{\partial\Psi}{\partial r}\right], \tag{12}$$

where $\bar{\lambda}$ is an arbitrary scalar function closely related to our function $\Lambda(\Phi)$ of Eq. (11), and Ψ is the poloidal flux. In this 1-D version we can compare our model to the Kadomtsev flux reconnection model [3].

III. NUMERICAL METHOD

We have developed a fully implicit code to implement our model in both 1-D and 2-D versions. In the 1-D version we advance the poloidal flux, Ψ, in time by solving Eq. (12). We normalize the equation to the resistive time. The value of the safety factor, q, can be found from the spatial derivative of Ψ and the current density by differentiating once again. We solve Eq. (12) by using an implicit finite difference technique and reduce the equations to block tridiagonal form. We integrate Ψ from the boundary inward with the boundary condition that the spatial derivative of Ψ is constant at the edge. This corresponds to the condition of keeping the total integrated plasma current constant.

In the 1-D case we compare this model to the Kadomtsev reconnection. To calculate the Kadomtsev reconnection we let the poloidal flux evolve due to resistive relaxation using Eq. (12) with $\bar{\lambda} = 0$. We convert to $m = 1$, $n = 1$ helical flux by subtracting the toroidal flux from the poloidal flux, then use the reconnection formulae given by Kadomtsev [3] to

5

calculate the helical flux after reconnection. We then compare this to the effect of triggering the sawtooth by letting $\bar{\lambda}$ be nonzero in Eq. (12).

In the 2-D version we advance the inverse q by solving Eq. (11) directly. We obtain the metric coefficients that appear in Eq. (11) by calling a 2-D MHD equilibrium program [15] that solves for the equilibrium, given the q-profile, at every iteration. The parallel current density is then found from a derivative of the inverse q. The implicit finite differencing technique is similar to that used in the 1-D case, and the boundary condition is to keep $q(edge)$ constant. We again normalize the equation to the resistive time using the total toroidal flux divided by the toroidal field at the plasma edge as the characteristic square length.

To model sawteeth we begin with some initial q-profile with $q_0 \approx 1$ and $q(r)$ increasing parabolically to the value at the outer radius, $q(edge)$. We let the current profile relax due to classical resistivity by solving Eqs. (11) or (12) with the hyper-resistivity term equal to zero. When q_0 reaches a predetermined threshold, typically $q_0 = 0.9$, we allow the hyper-resistivity term to come on by changing λ to a preselected nonzero form. The hyper-resistivity term will have the effect of flattening the current and q profiles in the region where λ is nonzero. When the value of q_0 reaches $q_0 = 1.0$ we set the hyper-resistivity term back to zero, and allow the profiles to again relax due to classical resistivity only. We then repeat the entire process several times until a steady-state sawtooth cycle is reached.

IV. RESULTS

In our 1-D cylindrical model we have found a form of the arbitrary functional coefficient, λ, with which our model very nearly matches the results of the Kadomtsev flux reconnection model. We use a resistivity profile given by $\eta(r) = \eta_0 exp(4.5r^2)$ corresponding to a resistivity that goes like $T^{-\frac{3}{2}}$ where the temperature profile is Gaussian. The hyper-resistivity profile is given by

$$\lambda(r) = \begin{cases} \lambda_0\left(1 - \left(\frac{r^2}{r_s^2}\right)\right)^\alpha & \text{for } r \leq r_s \\ 0 & \text{for } r > r_s. \end{cases}$$

The value we use for λ_0 is 775, and α is equal to 1.20. The value for r_s is determined by finding the point where the 1/1 helical flux is equal to the 1/1 helical flux at the center. It is inside this point where the Kadomtsev reconnection takes place and that the hyper-resistivity affects the flux. Outside of this point the flux is unchanged by both this model and the Kadomtsev model. Figure 1 shows the current profiles and q-profiles for both models immediately after triggering the sawtooth. Figure 2 shows how q_0 evolves in time according to both models. We see that for this form of $\lambda(\psi)$, the results of this model are nearly identical to those of the Kadomtsev model.

We can visualize how the current profile is affected by the hyper-resistivity as in Fig. 1.

6

From the form of the Ohm's law, Eq. (1), we see that if the magnitude of λ is large enough, then the hyper-resistivity term dominates the right-hand side of the equation. Furthermore, if λ is large, then the gradient of $j_{\parallel}/B$ must become small in order for the right-hand side of Eq. (1) to balance with the left-hand side. In other words, $j_{\parallel}/B$ becomes nearly uniform in the region where $\lambda(\psi)$ is large. Larger magnitudes of λ will produce more uniform profiles of $j_{\parallel}/B$. Just outside the region where the current profile is flattened, we see a sharp current reversal. This corresponds to the region where λ goes to zero. This negative current spike is a result of the inductive effect of the sudden mixing and equalizing of currents on adjacent magnetic surfaces [16]. In the region outside the current reversal the hyper-resistivity term is zero and has no effect on the equation. The profile is affected here only by classical resistivity; therefore the current profile in this region is essentially the same as it was before the sawtooth.

By choosing different magnitudes and functional forms for λ we can model sawteeth that are quite different in their precise form, but with the same qualitative behavior as Kadomtsev sawteeth. The Kadomtsev model can thus be thought of as one specific case of a more general range of sawtooth behavior which can be represented by our model. For instance, by changing the position of the λ cutoff, we can change the position of the current reversal and, therefore, determine how much of the inner region of the current profile is flattened. By changing the magnitude of λ we can specify how flat the resulting profile will be. If the magnitude is large enough, we can achieve a complete flattening of the current profile within this inner region. This is shown in Fig. 3. Once this limit in magnitude is reached, any further increase in magnitude or change in the functional form of λ will have no noticeable effect on the resulting profiles.

Figure 4 shows how the poloidal flux at the center, Ψ_0, evolves due to the effect of the sawteeth for both the Kadomtsev model and the hyper-resistivity model with λ equal to that used in Fig. 1. This illustrates how the volt-seconds from the Ohmic coils are 'consumed' by the sawteeth in both models. The effect of sawteeth on volt-second consumption is of considerable importance to the operation of tokamaks during the current flat-top phase, especially for Compact Ignition Tokamak designs and for long-pulse reactors [5].

The above-mentioned functional forms of the hyper-resistivity are all such that λ goes to zero exactly at some point and remains zero for all larger radii, i.e., these forms have a discontinuous derivative. Such a form is particularly well suited to match the Kadomtsev model, but may not be a good physical description of the hyper-resistivity. We can use forms of λ that are continuous in all derivatives, and produce qualitatively similar results as long as the hyper-resistivity approaches zero fast enough with increasing radius. For example, forms such as $\lambda(r)=\lambda_0 exp(-\alpha r^p)$ will produce behavior similar to the functional forms used above. The resulting current profile is not as flat and the current reversal is not nearly as sharp as in the Kadomtsev matching case, but the basic features are the same. Therefore, we know that it is not the discontinuity in λ or its derivatives that determines the overall form of the profiles. Again, we have the freedom to change λ_0, α, and p in order

to alter the precise form of the sawtooth behavior.

We extend our model to toroidal plasmas with cross-sectional shaping by using our full 2-D model. We use a form for λ that corresponds to that which we used to match the Kadomtsev model in our 1-D version. This is, therefore, a 2-D extension of the Kadomtsev prescription to a toroidal plasma with a shaped cross section. We have run cases for plasmas with circular cross sections and compared the results with those for plasmas with highly shaped cross sections.

We consider two cases for our 2-D model: (a) a circular cross-sectional plasma and (b) a plasma with a strongly shaped cross section (elongation=1.8, and triangularity=0.30). Figure 5 shows the current density profiles ($j_{\parallel}/B$ profiles) and the q-profiles for both cases at four times: at two times during the sawtooth crash, shortly after the sawtooth crash ($q_0 \approx 1.0$), and after some resistive relaxation and shortly before triggering the next sawtooth ($q_0 \approx 0.91$). The current profile of the elongated plasma evolves into a more hollow profile with the value on axis being significantly less than that at the peak. In fact, the value of the current on axis actually is higher during the first part of the sawtooth crash than it is just before the crash. This effect is much more pronounced for the elongated plasma than it is for the case with the circular cross section. To illustrate this, we have plotted the value of the current on axis, $j_{\parallel}(0)/B$, versus time in Fig. 6. We see that there is a significant difference in the development of $j_{\parallel}(0)/B$ between the circular plasma and the elongated plasma. Figure 7 shows the corresponding time evolution of q_0.

When the plasma recovers from a sawtooth crash, it begins with a fairly flat current profile. In the case of the highly shaped plasma, this current profile evolves into a slightly hollow profile during the initial resistive relaxation after the sawtooth. As this continues, the profile becomes more hollow, but the current that was forced outwards by the sawtooth begins to diffuse back towards the center. If this classical resistive diffusion continued indefinitely, the profile would, of course, evolve into its completely relaxed state, but the next sawtooth is triggered (at $q_0 \approx 0.90$) while the profile is still quite hollow. As the sawtooth is triggered, the hyper-resistivity flattens the current profile, and the current density near the axis is larger than that before the sawtooth when there was a local minimum on axis due to the hollow current profile. Therefore, the sawtooth causes a sudden, noticeable jump in $j_{\parallel}(0)/B$. There is a corresponding drop in q_0. As the hyper-resistivity continues to flatten the current profile, some of the current is redistributed towards the edge and the value of $j_{\parallel}(0)/B$ falls to the value it takes at the end of the crash. When the hyper-resistivity goes to zero at the end of the sawtooth crash, we have a nearly uniform current profile, and the whole process repeats itself. Keeping these steps in mind we can understand the evolution of $j_{\parallel}(0)/B$ in time as shown in Fig. 6(b). Furthermore, we can use the same reasoning to see why the evolution of $j_{\parallel}(0)/B$ in the case of the circular plasma, Fig. 6(a), looks so different.

The evolution of $j_{\parallel}(0)/B$ in the case of the circular plasma is not nearly so dramatic.

8

The current profile at the time that the sawtooth is triggered (see Fig. 5(a)) is not nearly as hollow as in the case of the highly shaped plasma. Therefore, when the hyper-resistivity begins to flatten the current profile, $j_\parallel(0)/B$ experiences only a small jump, and then immediately drops as the current density becomes more uniform across the profile. After the crash the current diffuses back towards the center due to classical resistivity, and $j_\parallel(0)/B$ increases again. Then the sawtooth is triggered again, and the whole process repeats itself. This gives a more conventional sawtooth pattern of $j_\parallel(0)/B$ for the circular plasma.

Figure 8 shows how the helicity, poloidal flux, and the total toroidal flux vary with time. We see that both the absolute and the relative change in the poloidal flux is substantially greater in the noncircular case, Fig. 8(b), than it is in the circular case, Fig. 8(a), even for the same relative change in q_0 during the sawtooth. The nearly discontinuous behavior of the poloidal flux in Figs. 8a,b is to be contrasted with the more gradual oscillations in the magnetic helicity, $K = \int_0^{\Phi_l} (\Psi - \Psi_l) d\Phi$, where the subscript '$l$' denotes the value at the limiter, or at the plasma edge. The helicity does not change discontinuously due to the direct action of the nonzero λ term, but does decrease due to the sharp current spikes created by the action of the sawtooth model. This decrease is compensated for, on the average, by the continued influx of helicity across the plasma boundary.

It is clear that all effects of the sawtooth oscillation are more pronounced in the noncircular cross-sectional geometry than in the circular cross section, although this result clearly depends on the assumption used here that the values of q_0 for which the sawtooth turns on and off are independent of the cross-sectional shape. The dominant effect of shaping the cross section is that for the same value of q at the limiter, the radius over which the current rearrangement occurs is substantially larger for the noncircular case than it is for the circular case. This is evident from comparing Figs. 5(a) and 5(b).

For cases with a larger value of q at the limiter, $q(edge)$, the sawtooth affects a smaller region of the profile. This results in more conventional sawtooth patterns for q_0 and $j_\parallel(0)/B$ even for cases with highly shaped cross sections. Here, however, we have considered a case with low $q(edge)$ to demonstrate the strong effects of cross-sectional shaping on the sawtooth behavior.

V. SUMMARY

We have developed a fully implicit MHD transport code in 1-D and 2-D versions that models the effect of the sawtooth instability using a hyper-resistivity term. With the 1-D version we can closely match the results of the Kadomtsev model, by a suitable choice of our parameters determining the form of the hyper-resistivity, λ. We can, given our freedom of this controlling function, also model sawteeth with behavior different from those of Kadomtsev. Thus, the Kadomtsev model may be regarded as a special case of the more

general model discussed here. Furthermore, our model has been extended to plasmas with shaped cross sections through our 2-D version.

With the 2-D model we have found that plasmas with strong cross-sectional shaping develop hollow current profiles after the sawtooth crash and have a larger fraction of their area affected by the sawtooth region. The plasmas that are more strongly shaped develop profiles that are more hollow. The sawtooth crash will initially increase the current density near the axis before current is redistributed outward by the hyper-resistivity. This results in an unusual sawtooth pattern for the current on axis, $j_{\parallel}(0)/B$.

Our form for the hyper-resistivity was chosen to be the form that matched the Kadomtsev model in the cylindrical limit, but it might be possible to develop a more self-consistent model by using a resistive stability code to calculate the eigenmodes and choose the form and magnitude of the controlling function, $\lambda(\psi)$, from the results of this stability analysis.

We have shown the utility of including a hyper-resistivity (or current viscosity) term in an MHD transport code in order to model MHD phenomena such as the sawtooth instability. We have also seen evidence that such a term may be useful in the modeling of magnetic islands and tokamak disruptions, and in the modeling of dc helicity injection through induced double tearing modes as in the dc helicity injection scheme on CDX [17].

ACKNOWLEDGMENTS

References

[1] S. von Goeler, W. Stodiek, and N. Sauthoff, Phys. Rev. Lett. **33** (1974) 1201.

[2] B. Coppi, L. Sugiyama, Comm. Plasma Phys. and Controlled Fusion **10** (1986) 43.

[3] B. B. Kadomtsev, Sov. J. Plasma Physics **1** (1975) 389.

[4] S. C. Jardin et al., Nucl. Fusion **27** (1987) 569.

[5] W. A. Houlberg, Nucl. Fusion **27** (1987) 1009.

[6] J. Schmidt and S. Yoshikawa, Phys. Rev. Lett. **26** (1971) 753.

[7] T. H. Stix, Nucl. Fusion **18** (1978) 353.

[8] A. R. Jacobson and R. W. Moses, Phys. Rev. A **29** (1984) 3335.

[9] A. H. Boozer, J. Plasma Physics **35** (1986) 133.

[10] E. Hameiri and A. Bhattacharjee, Phys. Fluids **30** (1987) 1743.

[11] H. R. Strauss, Phys. Fluids **29** (1986) 3668.

[12] A. Bhattacharjee and E. Hameiri, Phys. Rev. Lett. **57** (1986) 206.

[13] S. C. Jardin, N. Pomphrey, and J. DeLucia, J. Comput. Phys. **66** (1986) 481.

[14] A. H. Boozer, Phys. Fluids **24** (1981) 1999.

[15] J. DeLucia, S. C. Jardin, and A. M. M. Todd, J. Comput. Phys. **37** (1980) 183.

[16] T. H. Stix, Phys. Rev. Lett. **36** (1976) 521.

[17] M. Ono et al., Phys. Rev. Lett. **59** (1987) 2165.

Figures

Fig. 1. The current profiles and q-profiles for the Kadomtsev model and for the hyper-resistivity model in the cylindrical limit.

Fig. 2. The time evolution of q on axis, q_0, for both models.

Fig. 3. The current profiles and q-profiles for the Kadomtsev model and for the hyper-resistivity model with a large value of λ, which gives complete flattening.

Fig. 4. The time evolution of the poloidal flux on axis, Ψ_0, for both models. Note that the curve for the Kadomtsev model has been displaced downward, otherwise it would lie directly on top of the other curve.

Fig. 5. The current profiles and q-profiles at four different times during the sawtooth cycle for the 2-D model where we have (a) a circular plasma, (b) a highly shaped plasma (elongation $= 1.8$, triangularity $= 0.30$). The four times are shown on the time evolution of q_0 in Fig. 7. The radial variable r is the square root of toroidal flux contained within the surface, normalized to the value at the plasma edge.

Fig. 6. The time evolution of the current density on axis, $j_\parallel(0)/B$, for (a) the circular plasma and (b) the highly shaped plasma.

Fig. 7. The time evolution of the value of the safety factor on axis, q_0, for (a) the circular plasma and (b) the highly shaped plasma.

Fig. 8. The time evolution of the helicity, poloidal flux (ten times the difference between value at limiter and value on axis), and the total toroidal flux.
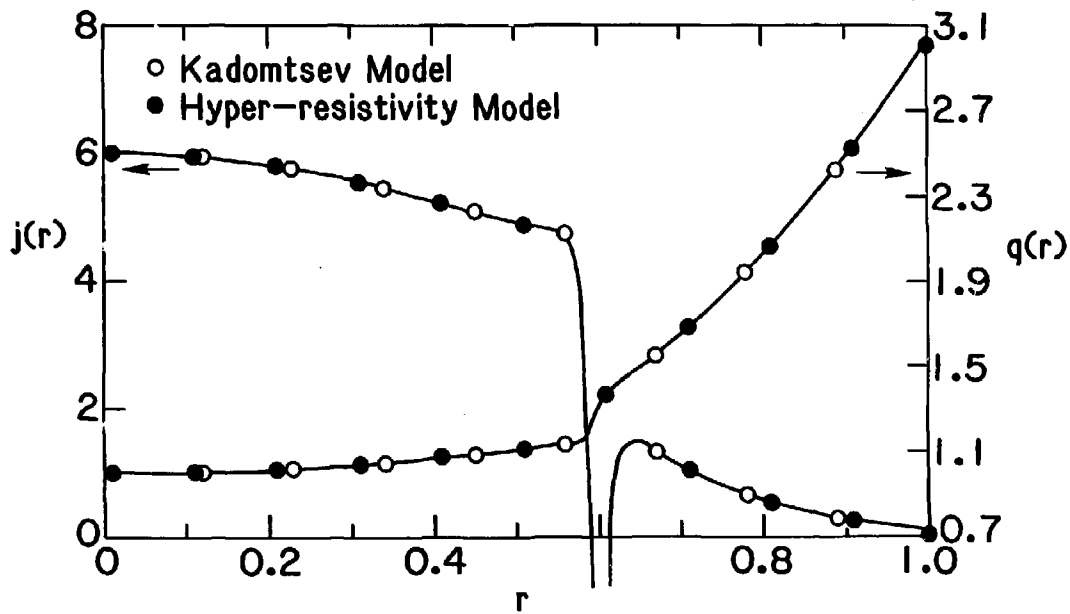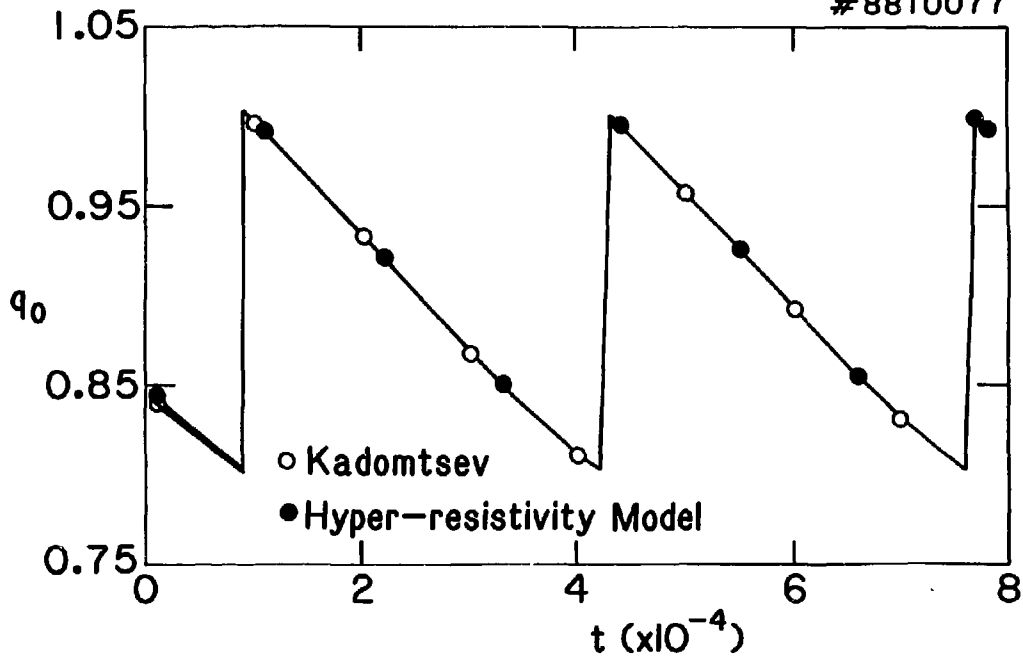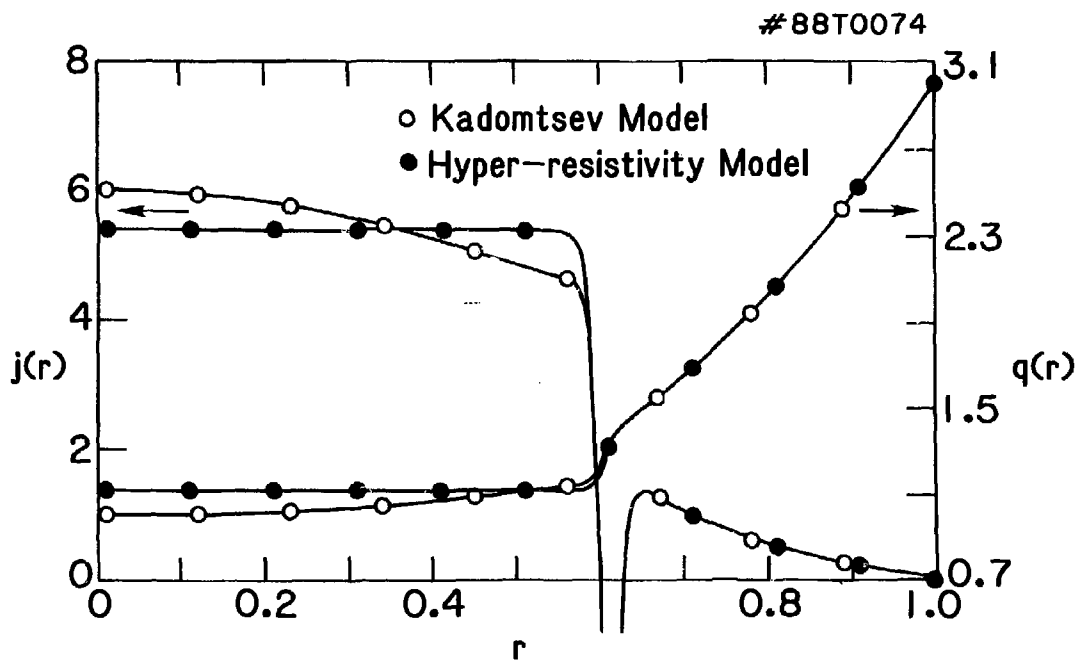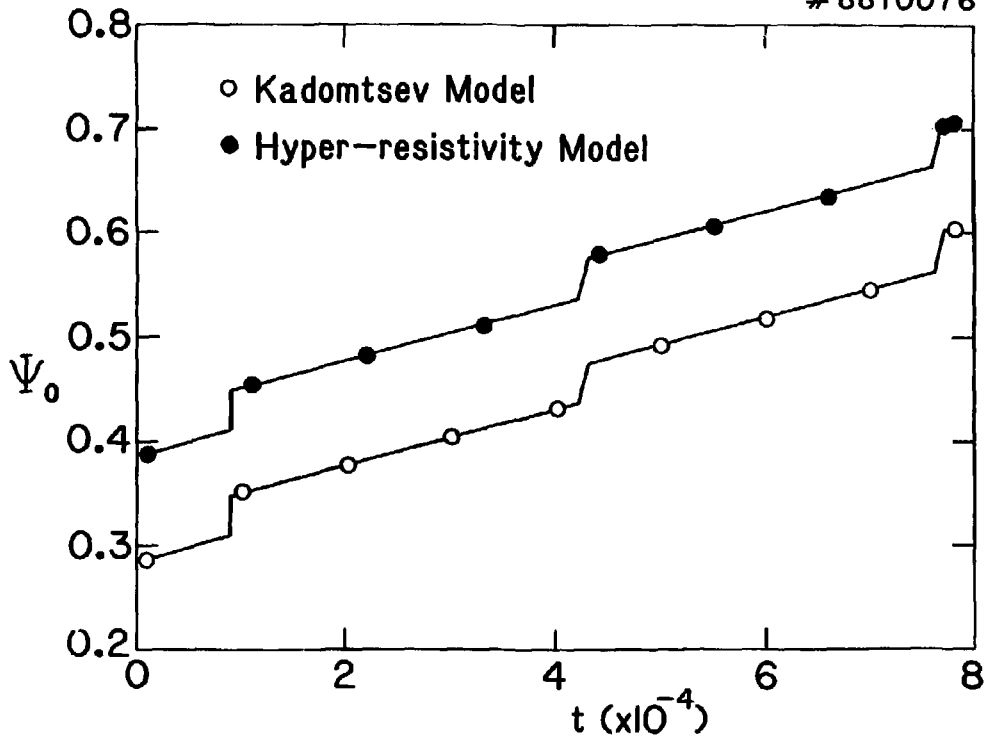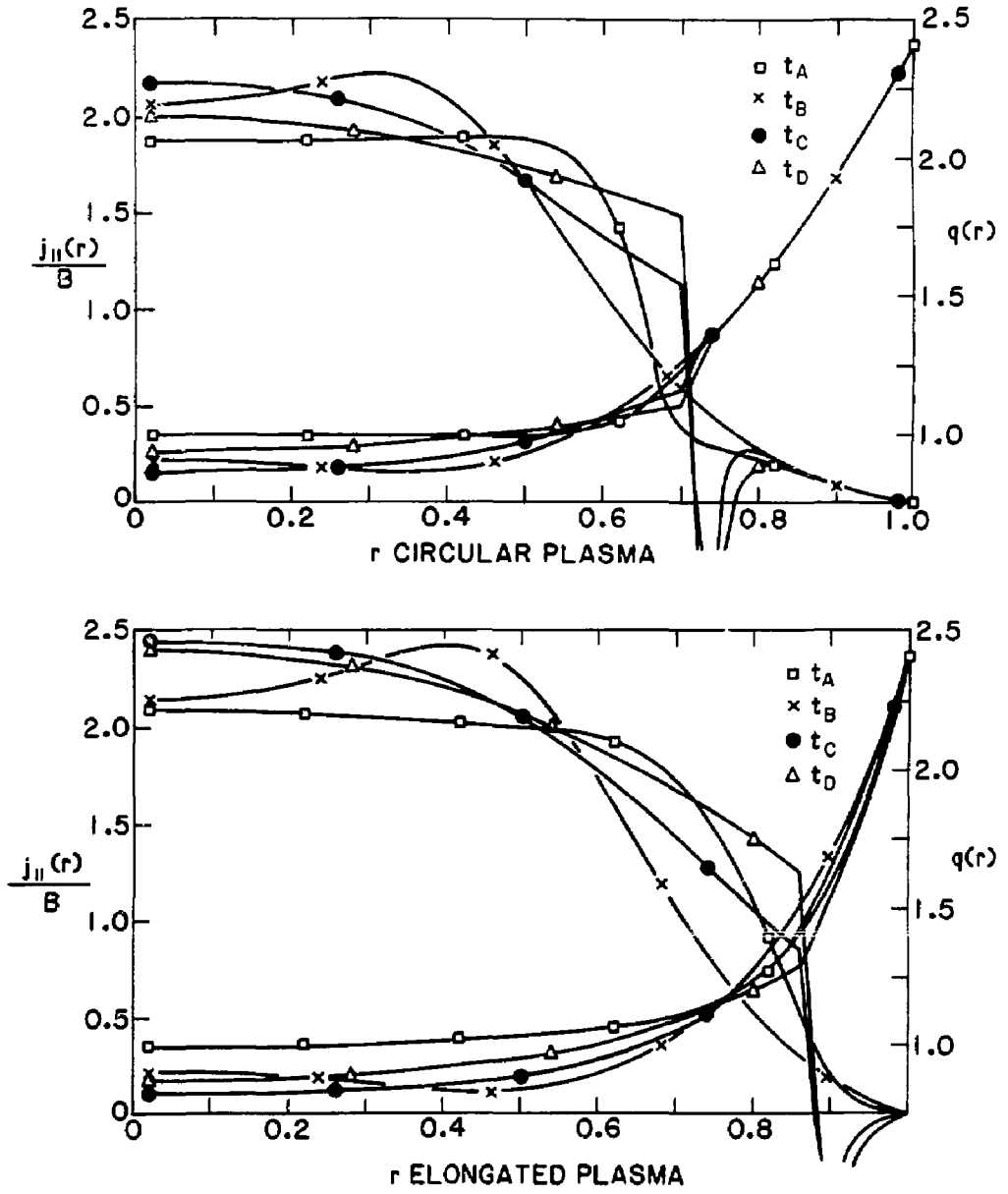
12

Fig. 1

#88T0077

14

Fig. 2

Fig. 3

Fig. 4

Fig. 5

Fig. 6

Fig. 7

(a)

FLUX

13

12

11

10

9

−10 (Poloidal Flux)

Helicity

Toroidal Flux

0   16   32   48   64   80

CIRCULAR PLASMA (t ×10^{-4})

(b)

FLUX

28

26

24

22

20

18

$\frac{2}{3}$ (Helicity)

−10 (Poloidal Flux)

Toroidal Flux

0   16   32   48   64   80

ELONGATED PLASMA (t ×10^{-4})
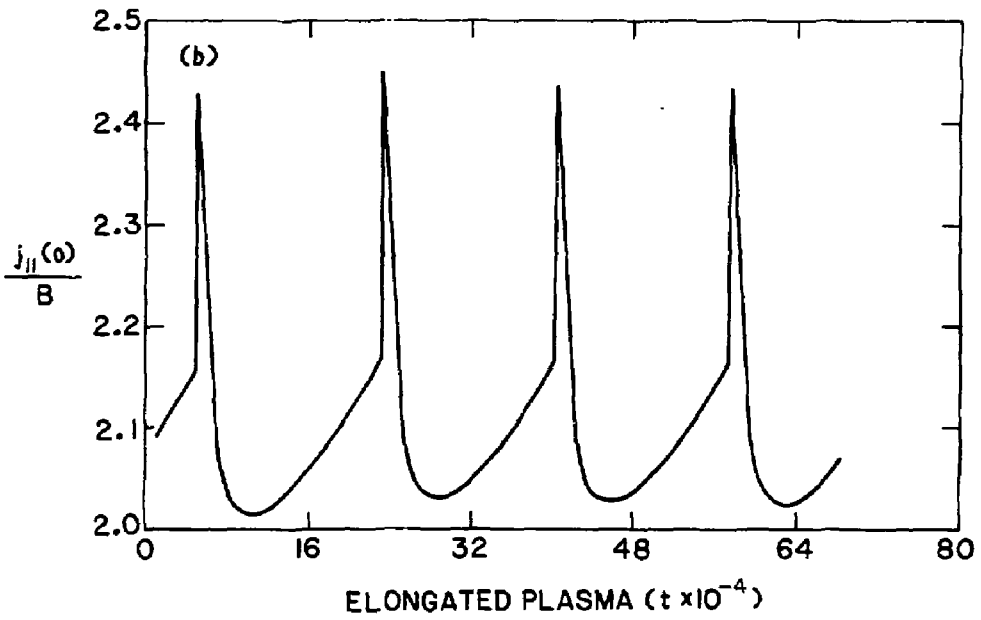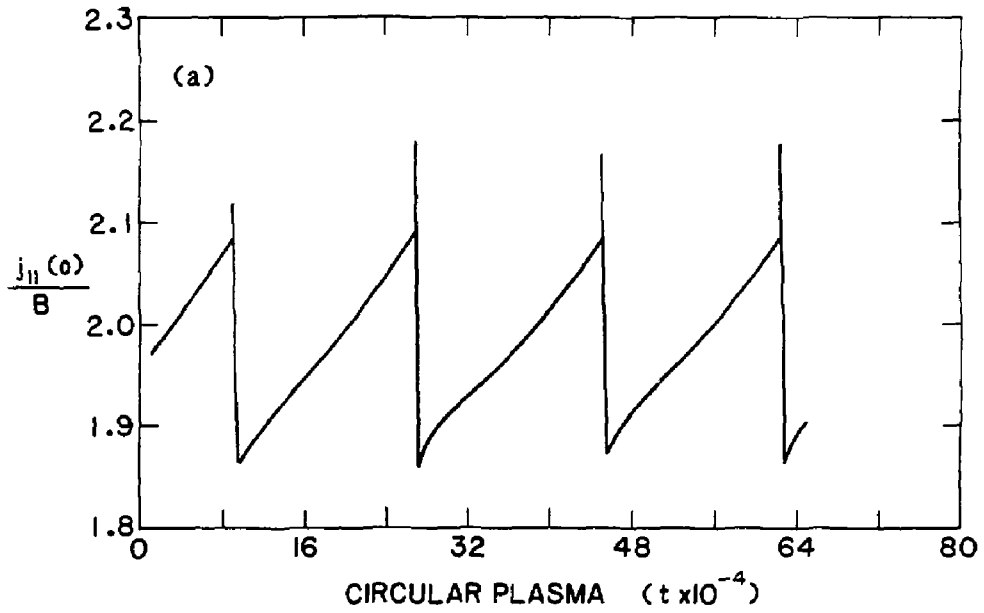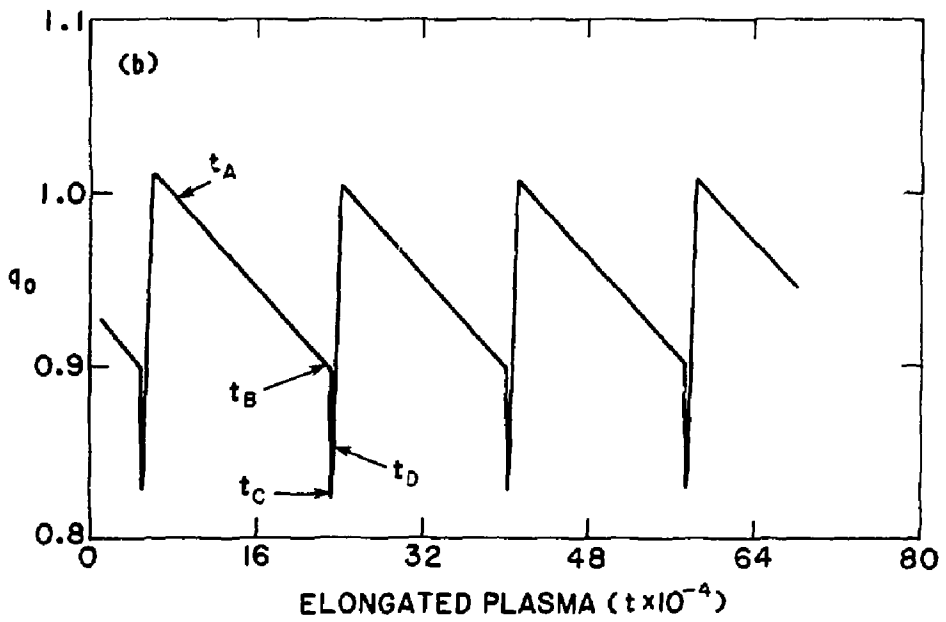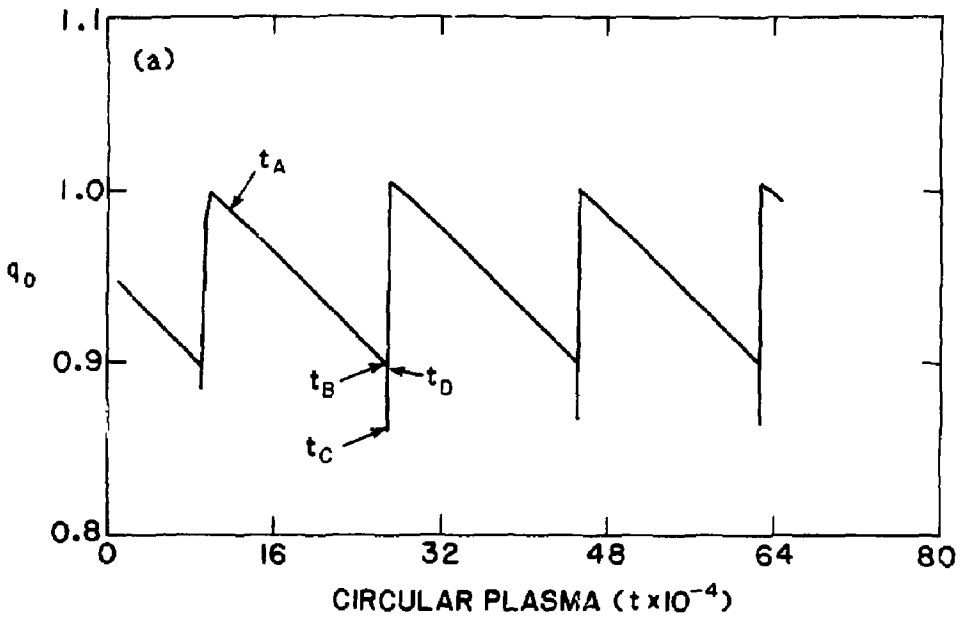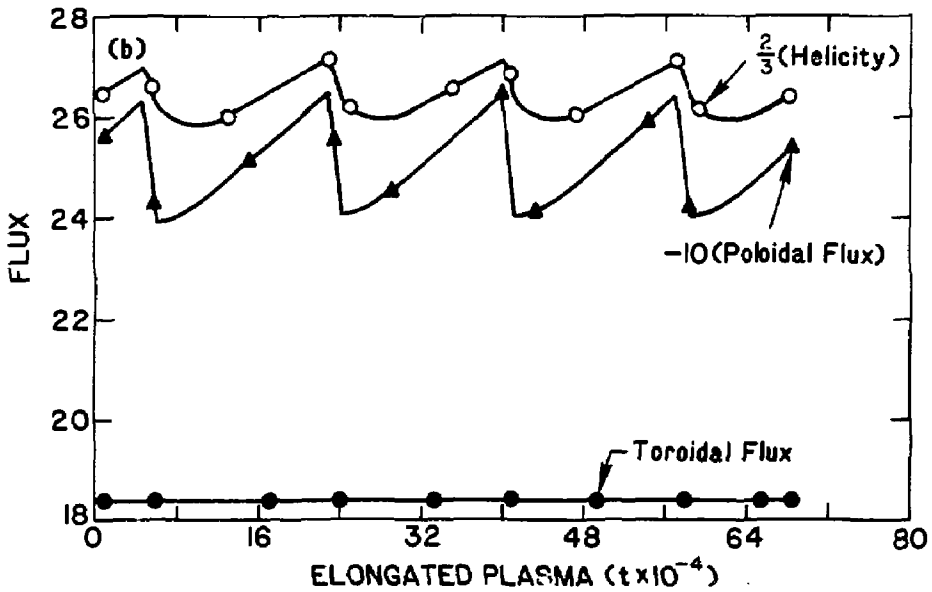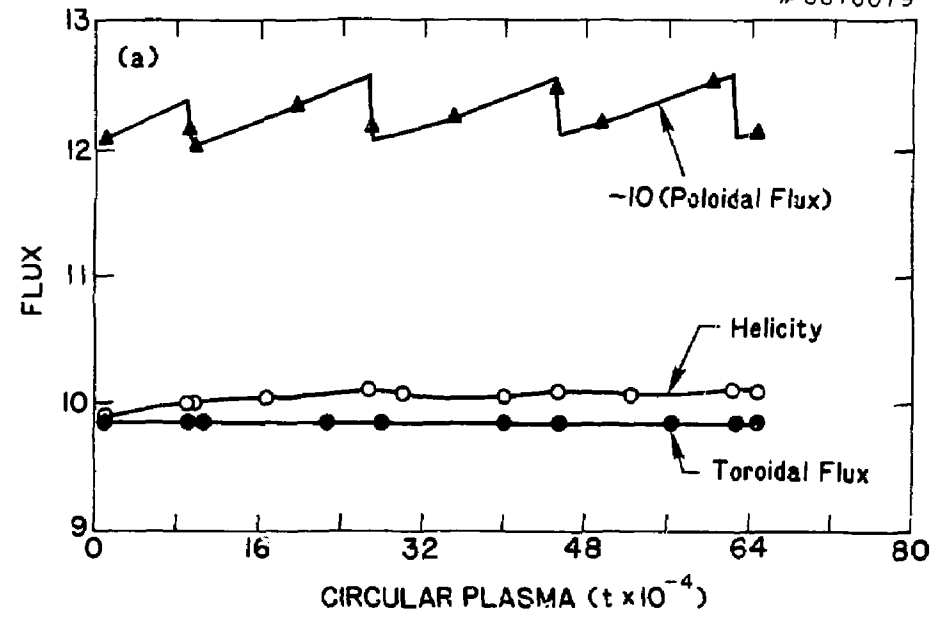
Fig. 8

Dr. Frank J. Paoloni, Univ of Wollongong, AUSTRALIA
Prof. M.H. Brennan, Univ Sydney, AUSTRALIA
Plasma Research Lab., Australian Nat. Univ., AUSTRALIA
Prof. I.R. Jones, Flinders Univ., AUSTRALIA
Prof. F. Cap, Inst Theo Phys, AUSTRIA
Prof. M. Heindler, Institut fur Theoretische Physik, AUSTRIA
M. Goossens, Astronomisch Instituut, BELGIUM
Ecole Royale Militaire, Lab de Phys Plasmas, BELGIUM
Commission-European, Dg-XII Fusion Prog, BELGIUM
Prof. R. Boucique, Laboratorium voor Natuurkunde, BELGIUM
Dr. P.H. Sakanaka, Instituto Fisica, BRAZIL
Instituto De Pesquisas Espaciasi-INPE, BRAZIL
Documents Office, Atomic Energy of Canada Limited, CANADA
Dr. M.P. Bachynski, MPB Technologies, Inc., CANADA
Dr. H.M. Skarsgard, University of Saskatchewan, CANADA
Dr. H. Barnard, University of British Columbia, CANADA
Prof. J. Teichmann, Univ. of Montreal, CANADA
Prof. S.R. Sreenivasan, University of Calgary, CANADA
Prof. Tudor W. Johnston, INRS-Energie, CANADA
Dr. C.R. James, Univ. of Alberta, CANADA
Dr. Peter Lukac, Komenskeho Univ, CZECHOSLOVAKIA
The Librarian, Culham Laboratory, ENGLAND
The Librarian, Rutherford Appleton Laboratory, ENGLAND
Mrs. S.A. Hutchinson, JET Library, ENGLAND
C. Mouttet, Lab. de Physique des Milieux Ionises, FRANCE
J. Radet, CEN/CADARACHE - Bat 506, FRANCE
Univ. of Ioannina, Library of Physics Dept. GREECE
Dr. Tom Mual, Academy Bibliographic Ser., HONG KONG
Preprint Library, Hungarian Academy of Sciences, HUNGARY
Dr. B. Dasgupta, Saha Inst of Nucl. Phys., INDIA
Dr. P. Kaw, Institute for Plasma Research, INDIA
Dr. Philip Rosenau, Israel Inst. Tech, ISRAEL
Librarian, Int'l Ctr Theo Phys, ITALY
Prof. G. Rostagni, Univ DI Padova, ITALY
Miss Clelia De Palo, Assoc EURATOM-ENEA, ITALY
Biblioteca, Instituto di Fisica del Plasma, ITALY
Dr. H. Yamato, Toshiba Res & Dev, JAPAN
Prof. I. Kawakami, Atomic Energy Res. Institute, JAPAN
Prof. Kyoji Nishikawa, Univ of Hiroshima, JAPAN
Direc. Dept. Large Tokamak Res. JAERI, JAPAN
Prof. Satoshi Itoh, Kyushu University, JAPAN
Research Info Center, Nagoya University, JAPAN
Prof. S. Tanaka, Kyoto University, JAPAN
Library, Kyoto University, JAPAN
Prof. Nobuyuki Inoue, University of Tokyo, JAPAN
S. Mori, JAERI, JAPAN
Librarian, Korea Advanced Energy Res. Institute, KOREA
Prof. D.I. Choi, Adv. Inst Sci & Tech, KOREA
Prof. B.S. Liley, University of Waikato, NEW ZEALAND
Institute of Plasma Physics, PFOPLE'S REPUBLIC OF CHINA
Librarian, Institute of Phys., PEOPLE'S REPUBLIC OF CHINA
Library, Tsing Hua University, PEOPLE'S REPUBLIC OF CHINA

Z. Li, Southwest Inst. Physics, PEOPLE'S REPUBLIC OF CHINA
Prof. J.A.C. Cabral, Inst Superior Tecnico, PORTUGAL
Dr. Octavian Petrus, AL I CUZA University, ROMANIA
Dr. Johan de Villiers, Fusion Studies, AEC, SO AFRICA
Prof. M.A. Hellberg, University of Natal, SO AFRICA
C.I.E.M.A.T., Fusion Div. Library, SPAIN
Dr. Lennart Stenflo, University of UMEA, SWEDEN
Library, Royal Inst Tech, SWEDEN
Prof. Hans Wilhelmson, Chalmers Univ Tech, SWEDEN
Centre Phys des Plasmas, Ecole Polytech Fed, SWITZERLAND
Bibliotheek, Fom-Inst Voor Plasma-Fysica, THE NETHERLANDS
Dr. D.D. Ryutov, Siberian Acad Sci, USSR
Dr. G.A. Eliseev, Kurchatov Institute, USSR
Dr. V.A. Glukhikh, Inst Electrophysical Apparatus, USSR
Dr. V.T. Tolok, Inst. Phys. Tech. USSR
Dr. L.M. Kovrizhnykh, Institute Gen. Physics, USSR
Nuclear Res. Establishment, Julich Ltd., W. GERMANY
Bibliothek, Inst. Fur Plasmaforschung, W. GERMANY
Dr. K. Schindler, Ruhr Universitat Bochum, W. GERMANY
ASDEX Reading Rm, IPP/Max-Planck-Institut fur
  Plasmaphysik, W. GERMANY
Librarian, Max-Planck Institut, W. GERMANY
Prof. R.K. Janev, Inst Phys, YUGOSLAVIA